01

Identification of optical magnetic resonances generated in a neon discharge by coherent transitions of spatially separated isotopically different atoms

© E.G. Saprykin

Institute of Automation and Electrometry, Siberian BranchRussian Academy of Sciences,
630090 Novosibirsk, Russia

e-mail: Saprykin@iae.nsk.su

Received on August 27, 2020
Revised on June 30, 2021
Accepted on October 25, 2021

Infrared (IR) transitions are identified in the neon spectrum in the range 0.76−15.8 μm, they generate resonances due to quadrature field synchronization of spatially separated isotopically different atoms. The use of numerical methods for the analysis of low-contrast IR resonances made it possible to estimate the previously unknown isotopic shifts of their parent transitions levels. A change in the amplitude sign of quadrature optical-magnetic resonances with a change in the isotopic shift sign of the transitions that generate them is found, and the dependence of the lifetime of such coherent atom pairs on the transitions wavelength is recorded, showing an unusual reaching the plateau as the wavelength decreases. It is assumed that this is due to expansion of the response time of the neighboring excited atoms of the isotopic pair to their fields interference.

Keywords: neon, IR transitions, field interference, coherent atom pairs.

DOI: 10.21883/EOS.2022.02.53210.223-21

Introduction

Previously, it was reported about discovery of unusual optical magnetic resonances, shifted relative to the magnetic field zero, in radiation of a neon discharge placed in longitudinal magnetic field with varying intensity [1,2]. They occur in a mixture of even neon isotopes and are not related to crossing of atom hyperfine structure (HFS) levels in the odd isotope ^{23}Ne [3,4]. These isotopic resonances (IR) appeared in magnetic fields compensating the isotopic shift (IS) of the lines, and were called optical-magnetic frequency crossing resonances (OMFCR) of the Zeeman line components. This phenomenon is little studied, and we will turn our attention to the mechanism of its occurrence, since earlier in the authors' publications its nature was interpreted ambiguously [5–10].

Initially, it seemed natural to associate the effect with crossing of the frequencies of linearly polarized σ-line components at $\Delta m = 2$, described by the expression

$$|H_r| = \frac{\Delta}{2g_m\mu_B}, \qquad (1)$$

where g_m — Lande factor, μ_B — Bohr magneton, Δ — in this case, IS, and we are talking about the interference of fields propagating across the magnetic field direction. However, identification of IRs (determination of the transitions that generate them) showed that the position of IRs in the magnetic fields scale is described by the expression with $\Delta m = 1$ [8][1]:

$$|H_r| = \frac{\Delta}{g_m\mu_B}. \qquad (2)$$

But for this, one should admit the possibility of interference of orthogonally polarized π- and σ-radiation components, which is impossible in wave optics. Namely in this connection it was suggested in [8] that the effect is due to the interference of quasistatic fields (QSFs) of overlapping near zones of isotopes, where the oscillations of dipoles? electric field contain both longitudinal and transverse components with respect to the magnetic field direction [12]. Therefore, in this zone there is a possibility of interference of QSFs generating orthogonally polarized wave fields.

When identifying the nature of OMFCR, interpretation of the most contrasting resonance in the region of 1300−1400 severely shifted in the magnetic field scale Oe (OMRFC-1350) turned out to be fundamental. According to (1) from its shift, ISs follow, exceeding the values registered in neon. And application (2) showed that this resonance is generated by the transition from the level $2s_4$ (Paschen notations) to the neon ground state [11].

In [10] 4 types of OMFCR are presented: in-phase, quadrature, difference, cooperative resonances, and a conceptually unified model of their origin is proposed, in which their shape is associated with different types of phase synchronization of emitter fields. Physically, it describes non-stationary interference of oscillations of two frequencies (amplitude beating) with time restriction of its registration

[1] Negative IRs lead to negative signs of magnetic fields and OMFCR sign change [11].

(averaging the beats over time), which depends on the frequency difference Ω for different stationary oscillations phase shifts.

The interference of QSFs of spaced isotope atoms begins as a result of synchronization of the atomic dipoles fields in the overlapping near zones of an atoms pair, transferring them to a superposition coherent state, and continues until step-like photon emission with recoil momentum transfer to the atom. In this case, the interference of pairs? QSF leads to deactivation of other excited atoms close to the pair with overlapping zones in resonance magnetic fields, converting the interference fields? intensities of the pairs into changes in the population of the neighboring excited atoms, accompanied by a decrease in the discharge radiation intensity along H.

In this connection, it becomes possible to obtain information about the duration of the fields interference of an isotope pair (about the lifetime of the isotope pair superposition state), and about the preparation time of a separate atom for photon emission. However, these possibilities can only be implemented if the characteristics of parent transitions are known: g-level factors and wavelengths, iė. after IR identification. In this case, the spectral filtering of radiation confirmed that the coherent process manifests itself in the form of an incoherent resonant change in the level population. As a result, these nonequilibrium population changes are transferred to many other levels of the gas-discharge plasma, which complicates IR identification, but opens the way to the study of phenomena generated by ultraviolet (UV) and infrared (IR) transitions beyond the spectral sensitivity of the radiation detectors used, if identification is implemented.

Previously, in the article [8], OMFCRs were identified based on visual estimates of their position in the magnetic field scale. Now the mechanism of resonance generation has become clearer, description models have been built, algorithms for programs for their numerical analysis have been developed, and it is possible to continue the work [8], returning to the analysis of archival experiments and to develop procedures for analyzing new experiments with OMFCR in the IR spectrum range.

Modeling resonances with trigonometric sinc functions

Isotopic resonances with the shape of the central structure, similar to the dispersion contour, were associated with initiation of forced oscillations of the isotopic partner with a phase lagging by $\pi/2$. In physics, this type of interference does not change the total intensity of the fields at the resonance center, since the field amplitudes squares add up during interference. Therefore, such IRs are called quadrature OMFCRs. When describing them, we proceeded from the general form of the trigonometric function $\mathrm{sinc}(x)$ with an arbitrary stationary phase difference of field oscillations $\Delta\varphi$ at time $t = 0$[2], displayed by the function F, which was obtained as a result of averaging over the time interval T_{int} of non-stationary interference of two harmonic electric fields of equal amplitudes, differing in frequencies and phases:[3]

$$F = \frac{\sin(\Omega T_{\text{int}} + \Delta\varphi) - \sin\Delta\varphi}{\Omega T_{\text{int}}},$$

$$\Omega = (\omega_1 - \omega_2), \quad \Delta\varphi = (\varphi_1 - \varphi_2). \tag{3}$$

Resonance is centered at the frequency difference zero Ω of oscillations of electric fields with frequencies ω_1 and ω_2, T_{int}) – - the duration of the fields beating averaging over the time of their coexistence. The resonance contour described by this function depending on the value Ω is a sharp structure (dispersive or peak) at the zero of the frequency splitting with a shape depending on $\Delta\varphi$. For induced radiation with phase lagging by $\pi/2$, the function F_q describing the quadrature OMFCR is a dispersion-like central structure:

$$F_q = \frac{\sin\left(\Omega T_{\text{int}} + \frac{\pi}{2}\right) - 1}{\Omega T_{\text{int}}}, \quad \Omega = (\omega_1 - \omega_2). \tag{4}$$

with decaying satellites of the constructive and destructive wings adjoining it during detuning. In this case, in contrast to phenomena like the effect Dicke with $\Delta\varphi = 0$, where the pair?s atoms must be slow enough so that their relative position does not have time to change during establishment of their internal state [13–15], quadrature OMFCRs are generated only by atoms moving relative to each other.

According to the experiment, quadrature OMFCRs are generated by applying a resonance magnetic field H_r, which ensures equality of frequency difference of emitters Ω and the isotopic shift of the transition corresponding to atoms that are immobile relative to each other. In this case, the total intensity of the fields does not change, since the squares of the field amplitudes are added. Deviation from frequency equality leads to the impossibility of stimulated radiation and to noncoherent combining of intensities. Therefore, no resonant singularity near frequency coalescence with immobile atoms should be generated. But if the atoms move in a direction transverse to the magnetic field with a relative velocity Δv that compensates for the detuning from resonance

$$k\delta v = \mu_B g(|H| - H_r), \tag{5}$$

[2] Standard trigonometric in-phase function with $\Delta\varphi = 0$ to describe the results [1,2] was originally used in the article [13], and then a clear demonstration of a similar sinc form in a helium discharge with residual traces of a neon isotopes mixture (Fig. 10 was found in [10]). But all subsequent experiments have shown that resonance forms with many satellites are the exception, not the rule.

[3] In this case, the field amplitudes were taken out of the integral sign, which is a greatly simplifying approximation for the near zone. But since the fields are averaged during atom motion, and the regions with the maximum fields? amplitude provides the main contribution, (3) provides good agreement with experiment.

due to the Doppler frequency shift, the resonance conditions for stimulated emission in magnetic fields $H \neq H_r$ are restored, maintaining a coherent bond between isotopes. In this case, in the vicinity of H_r, a quadrature OMRFC is formed, which is described by expression (4) in the frequency representation. In the derivative signal, it has an extremum on the field H_r with a resonance sign depending on the sign Ω in expression (4), i.e. on the IS sign of the parent transition.

But in quantum optics, the presence of quadrature interference in the radiation direction excludes the appearance of non-stationary interference (beatings) both in this direction due to the absence of a difference in the emitted frequencies Ω, and in the opposite direction due to the absence of backward radiation, since photons are emitted „needle-like". It is possible to understand the reason for beating appearance by considering the QSF interference of the radiation near zones propagating in accordance with the circular distribution diagram of the static dipole electric field. Here, the field that initiates synchronization propagates not only in the direction of the atom, which is forced to emit at the same frequency, but also in the opposite direction. In the same way, QSF of a forcedly radiating atom also propagates in both directions. However, if in the forward direction the Doppler shift, set by the difference in the emitters? velocities in the medium, compensated for the frequency difference introduced by the magnetic field (detuning from H_r), in the opposite direction, the Doppler shifts no longer compensate for the frequency difference, but double it, providing QSF frequency splitting of atoms Ω necessary for beating existence. In this case, the sign of the phase shift predicted by (4) should also change.[4] As a result, instead of the expected quadrature function (4) in the experiments, a function with a changed sign of the oscillations phase shift appeared:

$$F_q = \frac{\sin\left(\Omega T_{\text{int}} - \frac{\pi}{2}\right) + 1}{\Omega T_{\text{int}}}, \tag{6}$$

which in the first experiments caused bewilderment. In (6) the frequency splitting Ω corresponds to a certain relative velocity of isotopically different atoms in a plane orthogonal to the magnetic field, which compensates for the detuning from the resonance center. In this case, each atom of the impurity isotope finds a partner in the velocity distribution of atoms of the buffer isotope, which moves at speed that compensates for detuning from resonance. However, in each isotopic pair of a discharge cell with such a velocity difference, the spatial separation of isotopes is different, which leads to different amplitudes of the interfering fields. As a result, averaging of the pairs? fields over the cell volume corresponds to a certain averaged field, which is consistent with the approximation made in the derivation of (3).

[4] Speaking about the direction of the isotopic atoms? velocity vectors, we recall that we are talking about its projection in a plane orthogonal to the magnetic field direction.

Due to the reactive nature of QSFs that do not transfer energy and their rapid attenuation, it is impossible to detect the interference of moving oscillators pairs at the output of an atom ensemble. In a discharge, it manifests itself due to microresponse of the environment to the field of pair non-stationary interference, which can initiate decomposition of excited atoms of the close surrounding with appearance of new noncoherent reactive fields of these atoms already. The latter, in turn, initiate decomposition of the next layers of surrounding atoms, and so on, decreasing their concentration along the chain. To describe the response nonlinear nature, we used the simplest model of the medium response amplitude with a power parameter k_{st}:

$$I \sim ((1 + F_q)/2)k_{st}. \tag{7}$$

Increase in response in the constructive wing of the quadrature OMFCR is more efficient than in the destructive one, and this leads to deformation of the IR shape.[5] In the signal derivative, the observed peak form of the resonance can then be transformed into a form approaching the dispersive (in-phase) form. As noted earlier, satellites of the central structure of quadrature OMFCRs were found only in cooperative IRs generated by transitions with population inversion. The main reason for the suppression of satellites is the time spread T_{int} from pair to pair of isotopes due to different delays of the buffer isotope forced oscillation relative to the appearance of QSF, which initiates the process of the impurity isotope.[6]

When passing to cyclic frequencies (MHz), which are accepted in the literature for IS lines, and converting (6) to the magnetic fields scale, a function was used that takes into account the symmetry of the problem of the magnetic field sign (to reduce the computation time, all numerical coefficients including the factor 2 of the difference $(|H| - H_r)$, the Bohr magneton, the unknown g-degerate level factor, and T_{int} are combined into parameter $G_s = 1/(4\mu_B g_m T_{\text{int}})$, expressed in oersteds (Oe) and characterizing a specific OMFCR):

$$F_q(H) = \frac{\sin\left((|H| - H_r)/G_s - \frac{\pi}{2}\right) + 1}{(|H| - H_r)G_s}. \tag{8}$$

Finally, T_{int} (in ns) was calculated based on the results of fitting the width of G_s and resonance identification giving information about the g-transition factor using the expression

$$T_{\text{int}} = 1/(4\pi\mu_B g_m G_s) = 226.84/g_m G_s. \tag{9}$$

[5] In the first experiments, deformation of the quadrature OMFCRs was mistakenly taken for in-phase OMFCRs.

[6] In practice, the procedure for leveling the theoretical function derivative satellites by multiplying it by a near-rectangular cutting contour (see (8) in [11]) with a width parameter (kk) expressed in units of resonance width (G_s).

Experiment

The first identification of resonances centered on 1360 and 836 Oe (OMFCR1400 and OMFCR-900) assumed that they are generated by transitions to the ground state from levels $1s_2$ and $1s_{\{}4\}$ [2]. This was a consequence of the roughness of the results [16] on estimating IS of the ground state of neon (2 ± 3 GHz), which allowed for such an option. Subsequently, it turned out that in the visible neon spectrum, observation of IR generated by such transitions is impossible. This is a consequence of the fact that their levels decay directly into the ground state, bypassing the metastable states, which accumulate the resonant arrival of the nonequilibrium population generated by isotopic pairs and increase it compared to the equilibrium population in nonresonance magnetic fields.

To detect IR generated by radiation from the $1s_2$ and $1s_4$ levels, it was necessary to carry out special experiments with absorption of laser radiation from levels close to them, where the nonequilibrium population is directly transferred by inelastic collisions (specifically, from level $2p_4$ [11]). They showed small shifts of OMFCR$(1s_4-1S_0) = 200$ Oe and OMFCR$(1s_2-1S_0) = 70$ Oe, and the latter had the IR sign opposite to the other observed OMFCRs. This is a consequence of the negative IS of this transition and was the first experiment demonstrating the change of the OMFCR sign in such a process, which will be confirmed further on the example of IR transitions. This is one of the goals of this work.

OMFCR-1400 could not be identified in [8]. Three transitions to the ground state claimed this role, but the IS error of the latter did not enable to make a choice. The reason is that although in this case modern ground state IS estimates from [17] were used, they themselves were obtained using [18], which limits their accuracy. To identify the parent transition, the total probabilities of three transitions from these levels to metastable states and then upwards were compared. The transition $2s_4-{}^1S_0$ turned out to be a priority and, using it, IS of the neon ground state [19] was refined.

In this article, we will study the possibilities of identifying OMFCRs generated by IR transitions. Its complexity lies in the lack of information about their IS, the forces of the transition oscillators, and the Lande factors of highly excited levels. It is necessary to figure out to what extent the extrapolation estimates following from the known data for the underlying states can help in these matters. Since we are talking about a numerical analysis of the experiments that have already been described in [6,8], we will only repeat the key characteristics of the experiments, supplementing them with some details identified later.

Radiation intensity from the end face of a capillary (diameter 2.5 mm) with a direct current discharge, water cooled and placed in a longitudinal magnetic field, was studied as a function of its intensity, which varied within ± 1600 Oe. The discharge glow was recorded by a photodetector consisting of a silicon photodiode and a current-to−voltage converter. Spectral sensitivity region of the photodetector was $0.4-1.15\,\mu$m with a maximum at $0.9\,\mu$m. Infrared glass light filters (IRLF) and interference filters were used.

The automated control system for magnetic field scanning and signal recording ensured accumulation of many scanning passes of the integral signal and its derivative obtained using the modulation method and synchronous detection. An alternating magnetic field was created by an internal short solenoid located in the zone of uniform field of an external scanning solenoid. The amplitude of the magnetic field deviation with frequency of 450 Hz could vary. To increase discharge stability in the low current region, a low-current keep-alive discharge was used, and to reduce noise level, a microwave discharge which destroyed the striations was applied to the discharge sections located outside the solenoids.

The ^{20}Ne isotope enriched to 99.8%, the ^{22}Ne isotope with content of ^{20}Ne impurity of 7.8%, and their mixtures were used in the experiments. Gas pressure was measured with a thermocouple manometric lamp when gas was admitted into the cell with its subsequent cut-off by a cock and was of an estimated nature. This is a consequence of gas sorption and desorption by the heated porous cathode, which change isotope concentration in the discharge channel and isotope ratio depending on the gas sorbed by the cathode in previous experiments.[7]

To improve accuracy of the information obtained in experiments with OMFCR, it is important to correctly calibrate the magnetic scale, which establishes relationship between the current in the solenoid winding and the magnetic field intensity. This procedure can be easily performed provided that the magnetic field is uniform and is the same for all coordinates of the cell effective volume. In our articles, a large-diameter solenoid was used, and the magnetic field was non-homogeneous. Characteristics of magnetic fields generated by scanning solenoids and field deviations, as well as the emission OMR measurement procedure in the glow signal of the gas-discharge cell end face, are described in [5]. It is noted that the difference in magnetic scale calibration for different sections of the cell can lead not only to resonance shift, but also to deformation of their shape. The results of subsequent experiments [6,8–11] showed that the longitudinal spatial nonuniformity of magnetic fields can lead to a sharp dependence of the OMFCR characteristics on the discharge parameters and the detected radiation spectrum. Thus, if emission of strongly reabsorbed lines is detected, then the situation is possible when the signal is determined by the cell end closest to the photodetector with a reduced magnetic scale, and OMFCRs appear at high solenoid currents. Thus, their shift is overestimated compared to what is expected from IS of parent transitions. This circumstance dictates the need to detect radiation at low absorbing

[7] It was also possible to increase concentration of excited impurity atoms compared to the concentration in the ground state due to optical buffer isotope pumping [20].

transitions between highly excited low-populated levels, where the result is determined by the average magnetic field, using IR filters for this. Initially, the magnetic field coupling coefficient with the discharge current was set for its maximum at the solenoid center. The axes of magnetic field intensities in the figures of our publications are plotted on this scale. But in the numerical approximation of the diagrams, based on the data of the article [5], with IR filters, a correcting scaling factor k_m for transition from the maximum magnetic field to the average one, equal to 0.954, was used.

In terms of averaging magnetic field nonuniformities, experiments with absorption of monochromatic laser radiation should have given a result, that does not depend on line reabsorption. Such an experiment was set up in the article [11] at the $3s-2p_4$ transition in order to refine IS of the neon ground state. This is the case when there were no issues with resonance identification, and measurement accuracy needed to be improved, so special attention was paid to the magnetic field calibration. The experiments are notable in that in addition to OMFCRs recorded in the visible spectrum range, OMFCRs were observed and identified in the IR spectrum range. Comparison of their shifts in the magnetic field scale with the IS of their parent transitions led to a value of 0.955, close to the calculated one, and indicated a uniform spatial distribution of the OMFCR amplitudes generated by IR transitions. At the same time, the correction factor for shifting the Doppler contours at the $3s-2p_4$ transition, determined in additional experiments, was estimated at 1.01 ± 0.02. This fact indicated that the central part of the positive discharge column, which was previously considered to be homogeneous, provides predominant contribution to the signal. This unusual phenomenon is associated with saturation of transitions with the field of the discharge's intrinsic radiation, which increases level population and OMFCR amplitude in the central part of the cell with the discharge. It was later discussed in more detail in [21].

Results of numerical analysis of experiments

The main physical interest in the OMFCR characteristics is their widths G_s. They make it possible to estimate the residence time of isotope atom pairs in superposition states determined by the presence of interfering QSFs in their overlapping near zones. To do this, it is necessary to know the g-level factors and the wavelengths of the parent transitions. In 2014 we presented the first results on IR identification in a mixture of neon isotopes [8], where we appealed to the published ISs of neon lines. Then, thanks to a specific difference form, it was possible to identify the IR resonance of OMFCR-350, generated by the $3p_1-2s_2$ transition, (Fig. 5, 6 in [8]). In this article, by applying numerical processing of the experimental results and estimating the unknown IS levels following from the known IS lines, we succeeded in refining the position and widths of several more resonances, determining transitions claiming to generate them, and detecting the sign inversion of some of them.

The results of the presented experiments are shown in Fig. 1–5. In Fig. 1, the blue circles mark the contours with the amplitude sign corresponding to the positive IS of transitions, and the red circles — corresponding to the negative IS. The presence of IRs of different signs might be surprising if it had not already been shown earlier in [11] that when the IS transition sign changes, the resonances change sign too. Another surprising thing is why, among the published neon lines? ISs, a negative IS was found only for the $2s_4-{}^1S_0$ line?

In experiment 1 (Fig. 1), OMFCR-90, centered on a magnetic field of 91.8 Oe with a width of $G_s = 9.88$ Oe, is adjacent to IR of similar amplitude, but with opposite sign centered on 110 Oe with width of 8.1 Oe. Then, resonances of the opposite sign will be denoted by the negative sign of the OMFCR-(−110) magnetic field. The OMFCR parameters and assumed parent transitions are displayed in Table 1. Table 2 summarizes the expected ISs of levels with $J = 0$, 1 (numbers in brackets) that can generate IRs obtained by extrapolating the known ISs of highly excited levels to their zero values at the ionization thresholds. Bold text indicates the values obtained from the literature or during IR identification.

OMFCR data-90 of experiment 1 are given in the first line of Table 1. It is generated by the $4d_5-3p_3$ transition with wavelength of 2.8 μm and an oscillator force of $f = 0.22$. Identification reliability is determined by the fact that the ISs of the states $4d_5$ (106.86 MHz) and $3p_3$ (285.6 MHz) are calculated based on the published data on the lines?

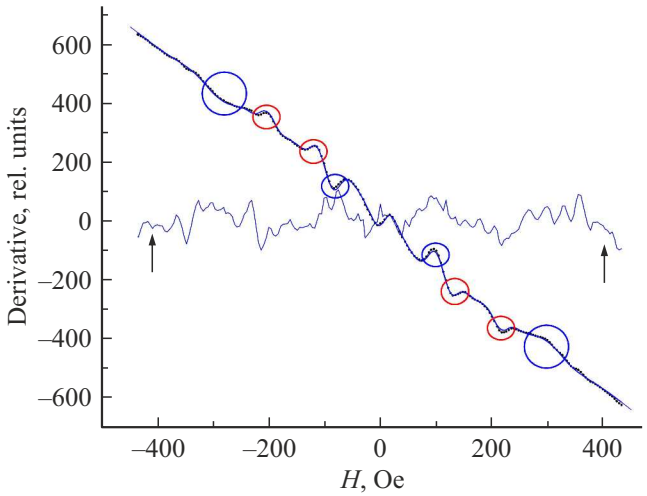

Figure 1. Experiment 1. OMFCRs, centered on 90, 110, 200 and 280 Oe. Neon-20, $p < 0.1$ Torr, $i = 29$ mA, deviation 26 Gs, IRLF LF-1, 22 scan region passes. The blue circles indicate OMFCR corresponding to positive IS, and the red circles — corresponding to negative IS. Horizontal curve — deviations of the experimental diagram from the model curve increased by a factor of 10 („residuals").

Table 1. OMFCR identification

№	OMFCR	experiment	H_r, Oe	Amplitude	k_{st}	kk, Gs	G_s, Oe	Parent transition	IS, Oe	λ, μm	g-factor	gG, Oe	T_{int}, ns	τ, ns	f
1	2	3	4	5	6	7	8	9	10	11	12	13	14		16
1 2	1 3, *a*	90	91.76	−1.1	1.42	3	9.88 13.48	$4d_5-3p_3$	91.8	2.8	1.391	13.74 18.75	16.5 12.08	34	0.22
3 4 5	1 3, *a* 3, *b*	−110	−110	0.695 1.156 0.147	1 1.6 1.22	3 3.22 3.06	8.10 9.45 8.2	$5d_5-4p_3$	−110	6.17	1.383	11.2 13.07 11.34	20.26 17.34 20.00	49.8	
6 7	1 5	−200	−198.9 −184	0.51 0.4	1 1	3 3	7.89 13.4	$5s_1'-4p_1$ $5d_2-4p_3$	−187 −188	5.85 6.06	0.809 0.791	6.44 10.06	35.2 21.4	96.6 34.7	
8 9 10	1 2 4	280	276.4 276 276.2	−0.94 −0.37 −2.34	1	3 10.5 6.87	17.74 15.58 10.76	$3p_2-2s_3$	277	2.31	1.397	24.78 27.13 15.03	4.57 10.42 15.08	114	0.5
11	2	130	129.3	−1.64	1.08	10.5	8.25 11.0	$5p_5-4s_3$	130	11.38	0.699	5.77 7.69	39.3 29.5	150	
12	5		129.6	−025	1.03	3.6	8.5					5.94	38.18		
13	2	50	50.7	0.43	1.1	10.5	4.55								
14	2	250	239	−0.24	1.66	10	5.26 7.46	$3d_6-2p_{10}$	250	0.75	1.984	10.43 14.8	21.72 15.4	18.4	0.14
15	4	250	255	−0.73 −0.51	1	3	6.46 9.15					12.81 18.85	17.7 12.04		
16 17	3, *a* 3, *b*	−10	−11.3 −7.56	0.39 0.33	1.02 1.00	3 2.85	2.37 2.14	$5s_2-5p_1$	−11.3 −7.6	15.76	1.315	3.12 2.81	72.8 80.8		
18	[10]	1330	1330	−1.69 −1.37	1.5 2.6	3	11 21	$2s_4-{}^1S_0$	1330	0.063	1.276	6.38 14.04	16.4 8.46	10.07	0.012

Note. τ — parent transition high level lifetime [23], f — parent transition degenerate level oscillator force [23].

ISs. The OMFCR-90 resonance also manifested itself in experiment 3 (Fig. 3, *a*) with width equal to 13.48 Oe (Table 1, line 2). Based on the widths, the interference time T_{int} was determined as (16.5−12.08) ns (Table 1). In this case, the value of 12.08 ns is in better agreement with the dependence of the interference time of the isotope pair fields on the transition wavelength (curve *1*, Fig. 6).

The $5d_5-4p_3$ transition with wavelength of 6.17 μm (Table 1, lines 3−5) is selected as a transition generating OMFCR-(-110). The unknown IS of level $4p_3$ was extrapolated from IS of levels $4p_{9,8}$ obtained from IS of transitions to levels $3s_5$ and $3s_4$ as 30 MHz, and the unknown IS of level $5d_5$ was determined based on the OMFCR-(−110) shift recorded in this experiment as 243.04 MHz $(g(5d_5) = 1.383)$. At the same time, it turned out to be close to the values of (238−242) MHz of levels $5d_2$, $5d_1''$, $5s_1$"" from the article [22], if an error in the IS sign of the transition lines from these levels to the levels $4p_{7,6,5}$, which are actually negative, is fixed in this article. The remaining 16 IR lines of this article were measured correctly, so finding the error and identifying its cause was not easy. As a result, lifetime of the superposition state of an isotopic pair at wavelength of 6.17 μm turned out to be equal to 20.26 ns. That is, as in reason, with a value greater than a value at the transition with wavelength of 2.8 μm. The same OMFCR-(−110) appeared in experiment 3 with width of 9.45 Oe, which leads to $T_{\text{int}} = 17.34$ ns (Fig. 3, *a*, Table 1, line 4), and with width of 8.2 Oe and $T_{\text{int}} = 20$ ns (Fig. 3, ,*b*, table 1, line 5). A candidate for generation of OMFCR-(−200) with shift −198.9 Oe (Table 1, lines 6, 7) is a transition $5s_1'-4p_1$ with wavelength of 5.85 μm. Here, if we set IS of level $4p_1$ equal to 30 MHz, as above, then with IS of level $5s_1'$ equal to 242 MHz (close to IS of levels 5*d*-), the OMFCR shift at $g(5s_1') = 0.809$ is expected to be close to $(-187\,G_s)$. But at the same time $T_{\text{int}} = 35.2$ ns, which is excessive when compared with the curve *1* in Fig. 6. Therefore, the data obtained for the resonance width (7.89 Oe) and the time T_{int} can not be considered acceptable, despite the admissibility of such an identification. A similar situation occurred with OMFCR-(−200), as well as with experiments 2 (Fig. 2) and 4 (Fig. 4) (not reflected in Table 1), also narrowed. It cannot be ruled out that the reason for data distortion over width of OMFCR-(200)

Table 2. Estimates of the IS of neon levels that form OMFCR (MHz)

s-levels		*d*-levels		*p*-levels	
$2s_4(1)$	**851.0**	$3d_6(0)$	**483.63**	$3p_{10}(1)$	350
$2s_2(1)$	**818.73**	$3d_5(1)$	**500.0**	$3p_7(1)$	350
$2s_3(0)$	**798.34**	$3d_2(1)$	**514.20**	$3p_3(0)$	**285.6**
$3s_4(1)$	**261.63**	$3s_1'(1)$	**398.58**	$3p_5(1)$	**255.2**
$3s_2(1)$	**172.73**	$4d_6(0)$	**101.47**	$3p_2(1)$	**256.4**
$3s_3(0)$	**147.33**	$4d_5(1)$	**106.86**	$3p_1(0)$	**222.6**
$4s_4(1)$	102.90	$4d_2(1)$	**125.43**	$4p_{10}(1)$	30
$4s_2(1)$	103.77	$4s_1'(1)$	**29.53**	$4p_7(1)$	**30**
$4s_3(0)$	**137.57**	$5d_6(0)$	**223.68**	$4p_3(0)$	**30**
$5s_4(1)$	67.4	$5d_5(1)$	**243.04**	$4p_5(1)$	**30**
$5s_2(1)$	**24.4**	$5d_2(1)$	**237.90**	$4p_2(1)$	30
$5s_3(0)$	30	$5s_1'(1)$	**241.80**	$4p_1(0)$	30
$6s_4(1)$	10	$6d_6(1)$	100	$5p_{10}(1)$	20
$6s_2(1)$	10	$6d_5(1)$	100	$5p_7(1)$	20
$6s_3(0)$	10	$6s_1'(1)$	75	$5p_3(0)$	10
				$5p_5(1)$	**10**
				$5p_1(0)$	10
				$6p_{10}(1)$	5
				$6p_1(0)$	5

Note. Numbers in brackets are total angular momentum of the level.

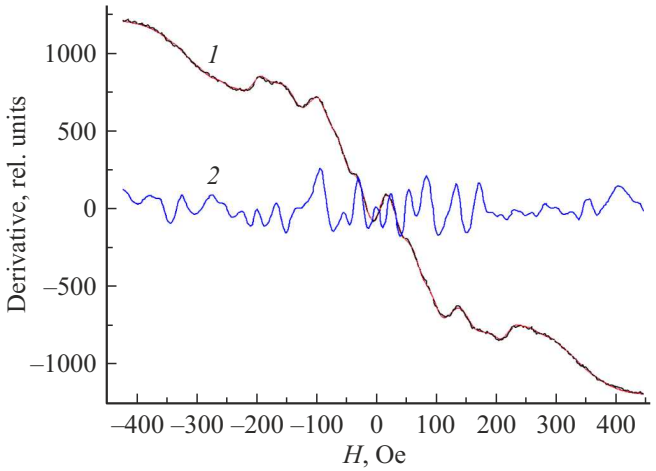

Figure 2. Experiment 2. *1* — OMFCRs, centered on 50, 130, 200, 240 and 280 Oe. Neon-20, $p \sim 0.1$ Torr, $i = 30$ mA, deviation 12 Gs, IRLF LF-7, 3 passes. *2* — deviations of the experimental diagram from the model curve increased by a factor of 10 („residuals").

may be IR with the opposite sign with a close shift that is not taken into account by the model. This OMFCR can be generated by the $3p_3-3d_2$ transition with wavelength of 5.67 μm, $g(3d_2) = 1.356$ and the expected shift of 190 Gs. The addition of two resonances with different signs can be the cause of sharpening of the narrower one. In this case (at close wavelengths) — a level with a smaller Lande factor, i.e. OMFCR-(−200). And only experiment 5 (Fig. 5, Table 1, line 7) with isolated OMFCR-(−200) and increased accumulation time showed more acceptable results both in terms of shift (−188 Gs), and width (11.7−13.4) Oe. As a result, the $5d_2-4p_3$ transition with wavelength of 6.06 μm, and $T_{\text{int}} = 21.4$,ns over the width upper limit is adopted as a parent transition. In this case, IS of level $5d_2$ was determined to be 237.9 MHz based on the results of measuring IS of the $5d_2-4p_7$ transition in [22].

The $3p_2-2s_3$ transition with wavelength of 2.31 μm was considered as a parent of OMFCR-280, the widest resonance of experiment 1 (Table 1, lines 8−10). In this case, IS of level $3p_2$ is known exactly based on IS measurements of neon lines (256.43 MHz), and IS of level $2s_3$, equal to 798 MHz, is determined based on the data of these measurements, which is in good agreement with the experimental estimates of IS of other levels 2*s*-. However, large width of OMFCR (17.74 Oe) may indicate the contribution of other transitions with shorter wavelengths, centered in close magnetic fields. Taking into account low contrast of OMFCR-280, there is no point in trying to resolve its structure in experiment 1 by numerical methods. However, it manifested itself - differently in other experiments, in particular, in experiment 2 (Table 1, line 9, Fig. 2) and in experiment 4 (Table 1, line 10, Fig. 4). Numerical analysis made it possible to extract OMFCR-250 from its structure, which led to narrowing of OMFCR-280 in experiment 4 (Table 1, line 10) and corresponded to the value of $T_{\text{int}} = 15.08$ ns, which was used for correction in Fig. 6. Visually invisible IR near 400 Oe finalizes the IR list of experiment 1, it is successfully contrasted in Fig. 6 of the article [8]. Here, the use of coefficients correcting the scale of the abscissa scale made it possible to estimate its shift as $\sim$ 380 Oe.[8]

Numerical analysis of experiment 2 (Fig. 2) identified new IRs in the vicinity of 130, 50 and 250 Oe (Table 1, lines 11, 13, 14). The OMFCR-130 shift was 129.3 Oe at width of $G_s = (8.25-11.0)$ Oe. The $5p_5-4s_3$ transition with wavelength of 11.38 μm was identified as a parent. There are no measured lines? ISs in the literature that would include levels $5p$, so we had to focus on ISs of levels $4p$ (30 MHz) confirmed above. Taking into account ISs of levels np tending to zero as their energy decreases, we adopted IS of level $5p_5$ to be less than 30 MHz (equal to 10 MHz). Then, using the resulting shift of OMFCR -130 and $g(5p_5) = 0.699$, we calculated IS$(4s_3) = 137.57$ MHz.

Based on the spread of OMFCR widths -130 (8.25-11.0) Oe, the transition time T_{int} $5p_5-4s_3$ was determined to be (39.3−29.5) ns with the value of 39.3 ns closer to the diagram *1* in Fig. 6. OMFCR-130 also manifested itself in experiment 4 with width scatter from 7 to 9.2 Oe, and in experiment 5 with width scatter from 8.17 to 8.76 Oe (Table 1, line 12). The latter is made with a signal accumulation time that is longer compared to the previous

[8] However, it was not possible to find candidates for generation of this OMFCR. Perhaps this is a faint transition between „hatched" and „non-hatched" neon levels.

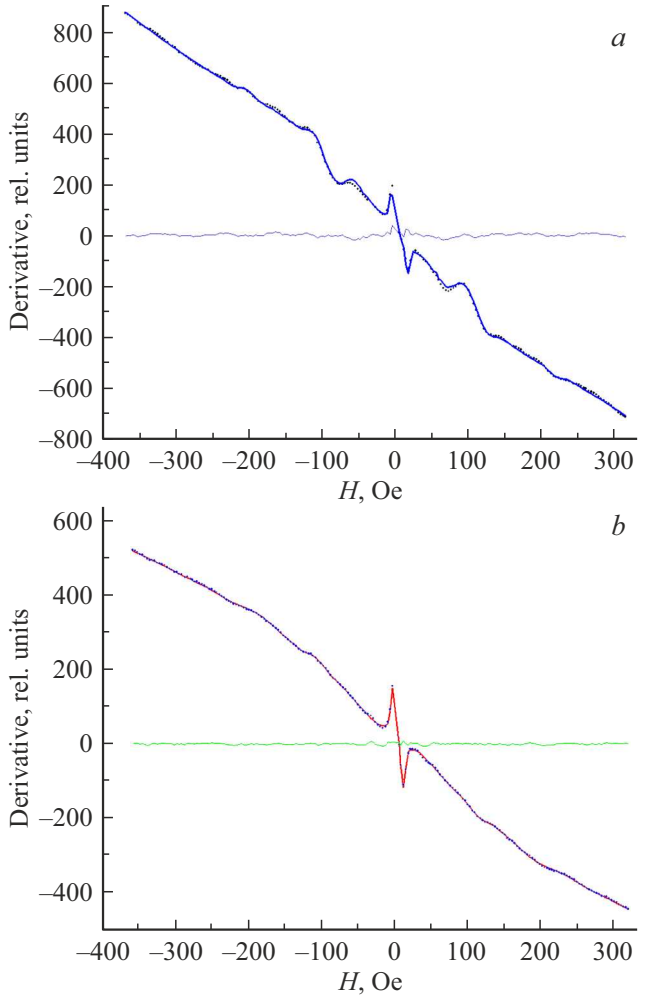

Figure 3. Experiment 3. LF 725 nm, neon-20, $p < 0.1$ Torr, $i = 29$ mA. Horizontal curve — deviations of the experimental diagram from the model curve („residuals"). *a*) OMFCRs, centered on 10, 90, 110, 200 Oe, deviation 17 Gs, 16 passes; *b*) OMFCRs, centered on 10, 110 and 200 Oe, deviation 10 Gs, 28 passes.

ones (16 passes versus three and five), so its $T_{\text{int}} = 38.18$ ns was also used to correct the curve *1* in Fig. 6.

Numerical analysis of the low-contrast OMFCR-50 (Table 1, line 13) determined its shift to be 50 Oe. In this case, it was also possible to approximate the negative OMFCR with other shift parameters, which calls reliability of the experimentally registered OMFCR-50 and its identification into question. Here, measurements are needed under other conditions, with a large IR contrast and with a smaller scanning step.

As a results of numerical analysis of experiment 2, within the wide structure of OMFCR-280, hidden OMFCR-250 was identified, centered on 233−239 Oe with width of (5.26−7.46) ,Oe (Table 1, line 14). It also appeared in experiment 4 at 248−260 Oe with width of (6.46−9.15) Oe (Table 1, line 15). The $3d_6-2p_{10}$ transition with wavelength of 0.75 μm with a known IS$(2p_{10}) = 1178$ MHz and the choice of IS$(3d_6) = 483.6$ MHz, close to the known IS of other levels $3d$- acts as a parent transition, providing maximum width of 9.15 Oe and $T_{\text{int}} = 12.04$ ns in accordance with the curve *1* in Fig. 6.

The next experiment 3 (lines 16, 17), carried out under close conditions for pressure and discharge current, but with different spectral filtering of radiation, identified OMFCR near 10 Oe. When using an IRLF light filter (LF)-7, the curve was similar to the curve in Fig. 2 in terms of the shape of the wide structure near the magnetic field zero. However, when setting SF 725 nm, it changed to a narrower one and of a different sign. Pumping of the mixture supplemented the experiment with a structure near 100 Oe (Fig. 3, *a*), similar to a dispersion contour, copying the same pair structure of the diagram of experiment 1. Therefore, there is no doubt that these resonances are generated by

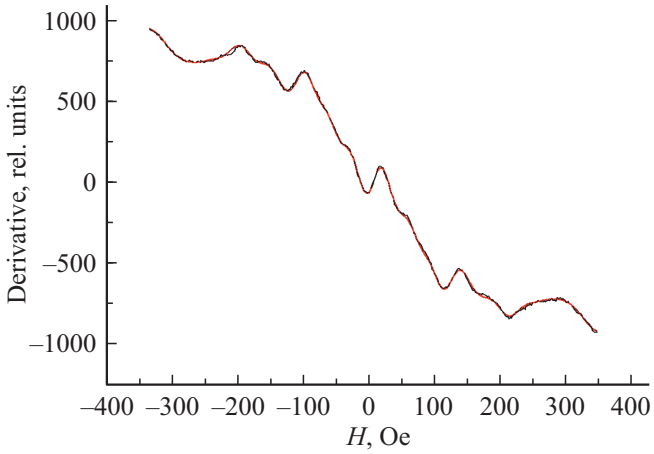

Figure 4. Experiment 4. OMFCRs, centered on 50, 130, 200, 250 Oe. Neon-20, $p \sim 0.1$ Torr, $i = 30$ mA, deviation 12 Gs, IRLF LF-7, 5 passes.

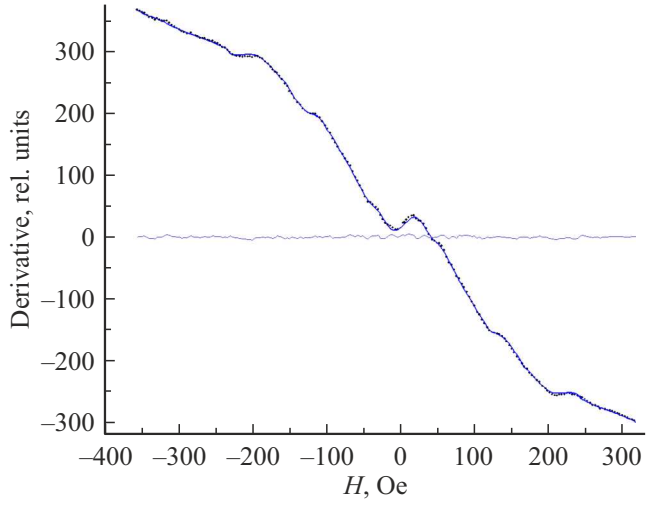

Figure 5. Experiment 5. OMFCRs, centered on 50, 130, 200 Oe. Neon-20, $p \sim 0.1$ Torr, $i = 27.6$ mA, deviation 11 Gs, IRLF LF-7, 16 passes. Horizontal curve — deviations of the experimental diagram from the model curve („residuals").

IR transitions between the same levels. However, these experiments were carried out without an IR light filter, so it cannot be guaranteed that the radiation of low absorbing transitions is also recorded with an interference light filter, and, indeed, it is possible to adopt the scale correction factor for the magnetic scale k_m corresponding to the average magnetic field (0.954). In this case, it is possible to determine k_m, using the resonance shifts recorded in experiment 1 as a reference value. Specifically, the shift of the more contrast OMFCR-90 was used. The obtained values of the parameter $k_m \approx 0.96$ turned out to be only slightly larger than those obtained with IR filters. It -appears that this is due to the fact that of the five lines that fall into the LF-725 bandwidth, two lines from levels $2p$ to levels $1s_{\{2\}}$ and $1s_4$ are so strongly absorbing that the signal is determined only by three weak transitions, for which the cell is transparent and the magnetic field is close to average. The results of OMFCR approximation of this experiment are shown in Fig. 3, *a* and in Table 1 (line 16). The shift of the new IR was determined to be 11.3 Oe c $G_s = 2.37$ Oe. The $5s_2-5p_1$ transition with $\lambda = 15.76\,\mu$m, with estimate of $\mathrm{IS}(5s_2) = 30.26$ MHz, set at $\mathrm{IS}(5p_1) = 10$ MHz expected for levels p- acts as a parent transition. In this case, the value $T_{\mathrm{int}} = 72.8$ ns was obtained, which is the maximum value for the empirical dependence of T_{int} on the wavelength.

In addition, in this series there was an experiment where only a narrow OMFCR near $H = 0$ was visually visible. However, due to the longer signal accumulation time (28 passes instead of 16), numerical processing identified the presence of two more IRs in it — OMFCR0-(−110) and OMFCR- (−200). The difference of this experiment is also in smaller deviation of the magnetic field (10 Gs instead of 17 Gs), which makes it possible to estimate the contribution of the deviation to the OMFCR-(−10) width. Therefore, its analysis was also carried out using the shift of OMFCR-(−110) determined in experiment 1 as a reference. In this case, two approaches were used: with scale calibration based on the results of experiment 3, Fig. 3, *a* (according to OMFCR-90), and according to OMFCR-(−110). The results turned out to be close and are shown in Fig. 3, *b* (Table 1, line 17). At the same time, the parameters k_m and k_p increased (0.988 and 0.999), and this affected shift and width of OMFCR-(−10). The main difference from the results in Fig. 3, *a* is that the OMFCR-(−10) shift turned out to be somewhat smaller (7.6 Oe), but still within the expected shift when correcting IS $(5s_2) = 30$ MHz to 24 MHz, and the width of interest was determined to be 2.14 Oe versus 2.37 Oe (Fig. 3, *a*). This leads to some increase in $T_{\mathrm{int}} = 80.8$ ns, but it does not fundamentally affect the course of the curve *1* in Fig. 6.[9]

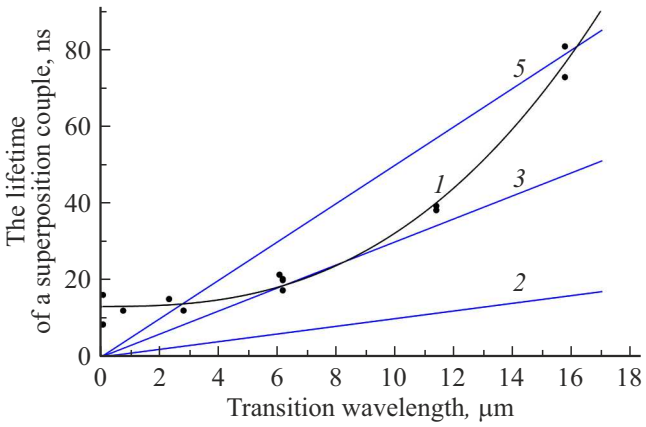

Figure 6. Dependence of the interference duration of isotope pair atoms on the transition wavelength: *1* is an experimental dependence described by the function $T_{\mathrm{int}} = 13.144 + 0.046\lambda^{2.455}$; *2*–*5* — times of isotope atom scattering to a distance λ in the direction orthogonal to the pair axis due to multidirectional atoms motion with velocities $\langle V_t\rangle$, $1/3\langle V_t\rangle$, $1/5\langle V_t\rangle$ respectively.

Thus, the experimental curve *1* in Fig. 6, as well as the data on the IS of highly excited neon levels, obtained as a result of identification of the presented OMFCRs, will be useful in further studies of IR generated by IR transitions. Their refinement will help to identify new OMFCRs and clarify the dynamics of spectroscopic transitions in the analysis of the fields of the atomic radiation near zone.

Finally, for comparison with T_{int} transitions in the UV spectrum region, the curve *1* in Fig. 6 contains the results of approximation of the quadrature OMFCR-1330 (Table 1 , line 18) generated by the $2s_4-{}^1S_0$ transition with wavelength of 63 nm from the article [10] (the points at y-axis). They, like the entire curve *1*, do not show drive towards the y-axis zero, which is due to the shortening of the existence time of QSF of atoms with an increase in the transition rate.

Discussion of results

One of the results of the article was the discovery of IRs with the amplitudes' sign opposite to those of the OMFCRs, generated by transitions in the visible spectrum range. Negative ISs were found in three IR transitions: $5s_1'-4p_1$ ($\lambda = 5.85\,\mu$m, IS = −211.8 MHz, $H_r = -187$ Gs), $5d_5-4p_3$ ($\lambda = 6.17\,\mu$m, IS = −213.04 MHz, $H_r = -110$ Gs), $5s_2-5p_1$ ($\lambda = 15.76\,\mu$m, IS = −24.36 MHz, $H_r = -7.8$ Gs). In addition, it was found that among the IR transitions measured in the article [22], there are three more transitions with negative ISs. These are the $5d_2-4p_7$ ($\lambda = 5.3264\,\mu$m, IS = −207.9 MHz), $5d_1''-4p_6$ ($\lambda = 5.3258\,\mu$m, IS = −207.9 MHz) and $5s_1''''-4p_5$ ($\lambda = 5.17\,\mu$m, IS = −211.8 MHz) transitions, whose ISs were erroneously identified as positive. These transitions do not have a nondegenerate level and cannot generate OMFCR, but they made it possible to refine the extrapolation estimates for IS of highly excited d-levels.

[9] Width of OMFCR-(−110), in this isolated experiment, was determined to be 8.2 Oe, which leads to the value $T_{\mathrm{int}} = 20.0$ ns (Table 1, line 5), consistent with the curve *1* Fig. 6. And for OMFCR-(−200), the width was determined to be narrower (11.5 Oe) compared to experiment 5, Table 1, line 7 (13.4 Oe), which is typical for this resonance (see above).

The results show that identification of OMRFCs generated by IR transitions, despite the lack of experimental data on the parameters of highly excited levels, is possible. This is helped by extrapolation of experimental data on the levels? IS to more highly excited ones.

An important result of the article was building of an empirical dependence of the interference time of the coherently clumped isotope pair?s fields (the lifetime of pair coherence) on the transition wavelength, represented by the curve *1* in Fig. 6. This makes it possible to use not only their shifts in the magnetic field scale, but also a comparison of their widths with the expected widths set by the transition wavelength when identifying OMRFCs. This is the practical utility of the diagram in terms of OMRFC identification. But there is still a question: what physical information about the superposition state of a coherently bound atoms pair this dependence displays, and to what extent it is subject to distortion in a moving atoms.

Even in the Dikke?s article [14] it was shown that interatomic quantum correlations of spatially close excited stationary atoms can lead not only to the acceleration of their joint decomposition, which he called superradiation, but also to its deceleration, later called subradiation. It was noted in the article [13] that correlations can be of both quantum and classical character. Being paraphrased into „the classical" processes in the generalized near zone, superradiation corresponds to the in-phase synchronization of the dipolar charge motion. In this case, the charges add up, the total current of the dipole pair and radiation velocity increase, and the time T_{int} decreases. Subradiation corresponds to antiphase synchronization of charge motion, when the charges are subtracted, the total current and radiation velocity decrease, and the time T_{int} must increase. In the case of quadrature synchronization with phase shift $\pi/2$, which we are studying, the total oscillating charge and current of dipoles do not change, and the time T_{int} in the limit is equal to the time during which a single atom is in the superposition state of transition between stationary states. In fact, it is, of course, less, since it is determined by the time of co-existence of the fields of two such atoms, which differs from pair to pair due to different delay of the forced field relative to the forcing one.

In addition, the course of this curve is also determined by the dependence of the isotopes? near zone overlap time on the relative velocities of the pair?s atoms. It was necessary to find out what finally determines the duration of field interference: the lifetime of the superposition state T_{int} or duration of near zone overlapping due to the motion of the pair's atoms. There are two mechanisms of motion influence here.

In the first case, we are talking about velocity projections lying in a plane orthogonal to the magnetic field and providing a Doppler shift $k\Delta v$, which compensates for detuning of the magnetic field from the resonance center:

$$k\Delta v = \mu_B g(|H| - H_r), \tag{10}$$

when passing to velocities

$$\Delta v = \mu_B g(|H| - H_r)\lambda/2\pi. \tag{11}$$

It can be seen from (11) that run of a distance λ equal to the region corresponding to the maximum amplitudes of isotopes? QSF takes time Δt, which does not depend on λ:

$$\Delta t = \lambda/\Delta v = 2\pi/[\mu_B g(|H| - H_r)]. \tag{12}$$

With detuning to the width G_s of OMFCR resonances introduced in (8) and associated with T_{int} by the relation $G_s = 1/(4\pi\mu_B g_m T_{\text{int}})$, we obtain, for $\mu_B = 1.404$ MHz/Gs, the estimate (in ns)

$$\Delta t = 637.2/(g_m G_s), \tag{13}$$

that is 2.8 times higher than T_{int} following from (9). Therefore, the time of crossing the isotopes? near zones can not serve as a factor limiting T_{int} from above.

The second situation is implemented when considering atom velocities projections directed orthogonally to the line connecting the atoms of an isotopic pair, i.e., along the magnetic field. Here, the isotope atoms relative velocity is determined by their thermal velocity, which can exceed the value given by (11), and there is no direct dependence on the magnetic field intensity. However, wavelength is included as a measure of the slope of the line connecting the isotope atoms with respect to the plane orthogonal to the magnetic field direction and its elongation. Therefore, here we can expect the action of the difference in the isotopes? transverse velocities, limiting T_{int}. But $\Delta t \sim \lambda/V_t$, and this is a linear function of wavelength, inversely proportional to the square root of gas temperature.

At the pair?s isotope velocities $\langle V_t \rangle \sim 0.5 \cdot 10^5$ cm/s, equal to the average velocity of neon gas atoms under normal conditions, but oppositely directed, Δt is represented in Fig. 6 by the curve *2*. This curve is below the curve *1*. With such a large relative difference in the isotopes? transverse velocities, the formation of coherent pairs with large times T_{int}, shown by the curve *1* in Fig. 6, is impossible. Such a possibility appears for pairs with a lower isotopes? transverse velocity. In Fig. 6, curve *3* corresponds to velocity by 3 times less, and curve *5* — by five times less than that for curve *2*. But when Δt tends to zero with decreasing λ intersects the curve *1*, this should lead to decrease in T_{int} on this segment of the absciss scale, whereas experimentally, a stationary value of ~ 13.5 ns is observed.

It was discussed above that growth of T_{int} can be interpreted as the transition of an isotope pair to a subradiative state with slowdown in atoms radiation decomposition, but this is surprising, since here we are studying OMFCR with quadrature synchronization of oscillations, therefore, a decrease in total charge and current of dipoles at antiphase synchronization, leading to the subradiation effect, should be absent. In addition, antiphase synchronization cannot be ensured with the help of near-field radiation QSFs, for which there is no delay effect, which promotes in-phase synchronization and prevents antiphase synchronization. Therefore,

it becomes necessary to involve the wave fields of the emerging photon, which, until energy accumulation $\hbar\omega$ are also essentially reactive fields, since they are not capable of energy transfer, but can provide oscillation synchronization. However, in the case of quadrature OMFCRs, the $\pi/2$ phase shift is due to the initialization of the stimulated emission of the isotopic partner and does not depend on the distance between them. In all cases, the OMFCR quadrature form (peak in the derivative) will be recorded. But in the case of antiphase synchronization, the derivative should have a dispersion-like form [10], which is not observed.

This indicates the presence of an effect whose nature is unclear. There is an assumption that tending of the curve *1* to a nonzero limit with shortening of wavelength is not associated with subradiation, but is due to lengthening of the time of non-coherent response of the surrounding excited atoms to the coherent pair interference field. I.e. deactivation of nearby excited atoms, which grows with an increase in the transition probability in proportion to the frequency cube and extended in time due to the successive connection of more and more atom layers to the process. This time is determined by the rate of deactivation process propagation, which depends on the transition probability, wavelength, and cell size.

Nonlinearity of increase in the superposition pair lifetime with increase in wavelength, which should acquire a linear character above certain wavelengths, also bepuzzles. It is possible that these wavelengths were not reached in these experiments. And to reduce the nonlinear response duration, the concentration of excited atoms or cell diameter should be reduced, which, of course, will reduce the IR amplitude. To clarify these possibilities, development of a theoretical process model and additional experiments with OMFCRs generated by both IR and UV transitions are required.

Conclusion

Thus, the results obtained laid the foundation for identification of new IRs using the experimental dependence of the quadrature OMFCR widths on the wavelength of the transitions that generate them, but at the same time raised questions about the reasons for its formation.

It was found in the article that the residence time of the superposition state reaches a plateau in the region of short wavelengths with time much longer than expected one for high transition frequencies. This was associated with an increase in the duration of the medium response to the isotope pair interference field. The probability of deactivation of the surrounding excited atoms increases cubically with an increase in the transition rate, and depends on the concentration of excited atoms and the cell size. But what can be the reason for the large times T_{int} in the region of long-wavelength IR-transitions? Here both the frequencies are low and the population of highly excited levels is small. In this regard, the following questions arise.

What determines the experimentally measured finite times T_{int} for a isotope pair to stay in a coherently bound state, from which follows the finiteness of the times for atom transition from one stationary state to another?

To what extent can they be related to the extended rather than step-like nature of atomic transitions predicted by Heisenberg?[10]

What role do the reactive fields of the atom radiation near zone play in identification of this extension?

These issues are beyond the scope of this article and will be discussed later.

Funding

The article was carried out within the framework of priority studies of the Siberian Branch of the Russian Academy of Sciences (Program II.10.2).

Acknowledgments

The author is grateful to V.A. Sorokin, who was a co-author when obtaining the results on IR identification in the article [8], to A.M. Shalagin and S.L. Mikerin for supporting the article, L.V. Ilyichev for remarks made when reading the article.

Conflict of interest

The author declares that he has no conflict of interest.

References

[1] E.G. Saprykin, V.A. Sorokin. In: *IVth Int. Symposium Modern Problems of Laser Physics* (Novosibirsk, 2004), p. 240.
[2] E.G. Saprykin, V.A. Sorokin. In collected volume: *Proceedings of the IV International Conference ?Problems of Fundamental Optics?* (St.-Petersburg, 2006), p. 173.
[3] M.P. Chayka. *Interferentsiya vyrozhdennykh sostoyaniy* (L.: Izd-vo LGU, 1975) (in Russian).
[4] E.B. Alexandrov, G.I. Kvostenko, M.P. Chayka. *Interferentsiya atomnykh sostoyaniy* (M.: Nauka, 1991) (in Russian).
E.G. Saprykin, V.A. Sorokin. Opt. i spektr., **109**, 573 (2010) (in Russian).
[6] E.G. Saprykin, V.A. Sorokin, A.M. Shalagin. ZhETF, **143**, 622 (2013) (in Russian).
[7] V.A. Sorokin. In: *Sixth Int. Simposium Modern Problem of Laser Physics* (Novosibirsk, 2013), p. 241–242.
[8] E.G. Saprykin, V.A. Sorokin. Opt. i spektr., **117**, 18 (2014) (in Russian).
[9] E.G. Saprykin, V.A. Sorokin, A.M. Shalagin. Quant. electron., **48**, 827 (2015) (in Russian).
[10] E.G. Saprykin. ZhETF, **149**, 251 (2016) (in Russian).
[11] E.G. Saprykin. Opt. i spektr., **122**, 568 (2017) (in Russian).
[12] R. Feynman, R. Leighton., M. Sands. *Feynman Lectures on Physics.* Vol. 5. Electricity and magnetism. (M.: Mir, 1977).
[13] L.V. Ilyichev. ZhETF, **131**, 30 (2007) (in Russian).

[10] Questions of the spectroscopic transition dynamics in the Heisenberg representation are considered in Section 4.4 of the monograph [24].

[14] R.H. Dicke. Phys. Rev., **93**, 99 (1954).
[15] A.A. Makarov, V.S. Letokhov. ZhETF, **124**, 766 (2003) (in Russian).
[16] W. B. Westerveld, J. van Eck. J. Phys. B., **12**, 377 (1979).
[17] K.S.E. Eikema, W. Ubachs, W. Hogervorst. Phys. Rev. A., **49**, 803 (1994).
[18] H. Shober. Pys. Zs., **40**, 77 (1939).
[19] E.G. Saprykin. Opt. i spektr., **120**, 222 (2016) (in Russian).
[20] E.G. Saprykin. Opt. i spektr., **127**, 179 (2019) (in Russian).
[21] E.G. Saprykin. Opt. i spektr., **123**, 285 (2017) (in Russian).
[22] J.C. Keller, J.F. Lesprit. Physica., **64**, 202 (1973).
[23] P.F. Gruzdev. *Veroyatnosti perekhodov i radiatsionnyye vremena zhizni urovney atomov i ionov* (M.: Energoatomizdat, 1990) (in Russian).
[24] J.D. Macomber. *The Dynamics of Spectroscopic Transitions* (New York–London–Sydney–Toronto: John Wiley and Sons, 1976). [J.D. McComber. *Dynamics of spectroscopic transitions* (M.: Mir, 1979).]